Acta Metall. Sin. (Engl. Lett.), 2014, **27**(2), 253–258
DOI 10.1007/s40195-014-0056-0

Spin-Relaxation of NiO Encapsulated Gd_2O_3 Core–Shell Nanoparticles

A. Rajesh · M. Manivel Raja · K. Gurunathan

Received: 29 August 2013 / Revised: 27 November 2013 / Published online: 19 April 2014

Abstract Nickel oxide encapsulated gadolinium oxide (Gd_2O_3/NiO) core–shell nanoparticles (Nps) has been synthesized by polyol method and analyzed by transmission electron microscopy. The particle size is found to vary from 25 to 35 nm. Raman spectra show the gadolinium oxide core material peaks are found to be diminished by the mass effect of the NiO shell material. The dynamics of the magnetic moment has been studied with the help of temperature dependent electron paramagnetic resonance (EPR) spectroscopy. Peak-to-peak line width (ΔH_{pp}) value of the EPR spectra increases with decreasing temperature. Temperature dependence of line width shows the dominance of spin–lattice relaxation in these systems, and it can be used as T_1 contrast agent. Spin number estimated from EPR studies increases with the decrease of the temperature. The interfacial exchange coupling between the core and shell region is found to be existing at very low temperatures as determined by EPR studies in this non-magnetic/antiferromagnetic (NM/AFM) core/shell nanosystem. The effects of the temperature on the magnetic properties of the Gd_2O_3/NiO core/shell NPs and the underlying mechanism have been discussed.

KEY WORDS: **Nanocomposite; Magnetic material; Raman spectroscopy; Electron paramagnetic resonance (EPR); Spin-relaxation**

1 Introduction

In recent years, science and technology have considerably developed and have created various nanomaterials such as nanoparticles [1], nanotubes [2], nanofilms [3, 4], graphene [5] and nanoporous materials [6]. Among them, the core–shell nanoparticles (Nps) with magnetic components have attracted much interest in recent years both in fundamental research [7] and practical applications [8]. The core–shell Nps are also been widely investigated for biological applications example drug delivery, cell labelling and magnetic resonance imaging (MRI) etc. [9]. These core/shell Nps can be used as a contrast agent to improve the visualization of MRI images, which is a diagnostic technique widely employed due to its capability to distinguish healthy tissues from affected tissues. Core/shell Nps can enter the cells and they act as efficient contrasting agent due to its better spin–lattice relaxation time [10, 11].

The use of contrast agent for MRI depends on the ability of the agent to shorten the relaxation time (T_1 and T_2) of water's protons. Each distinct tissue type has unique relaxation rates ($1/T_1$ and $1/T_2$) and a proton density, which affects tissue contrast and image interpretation [12]. Relaxation rates $1/T_1$ and $1/T_2$ measure the rate that molecular spins after being perturbed by the radio-frequency wave inside a magnet return back to their energy

Available online at www.springerlink.com/journal/40195

A. Rajesh · K. Gurunathan (✉)
Department of Nanoscience and Technology, Science Block, Alagappa University, Karaikudi 630 004, India
e-mail: kgnathan27@rediffmail.com

M. Manivel Raja
Defence Metallurgical Research Laboratory, Kanchanbagh PO, Hyderabad 500 058, India

equilibrium states. T_1 is called spin–lattice relaxation time that is the time needed for spins and their environment (dubbed "lattice") to reach energy equilibrium. T_2 is called spin–spin relaxation time and it is time for spins themselves to reach equilibrium after radio frequency wave perturbation [13]. Ahren et al. [14] reported that Gd_2O_3 nanoparticles shown a high relaxivity compared with commonly used gadolinium (III) chelates, indicating that Gd_2O_3 particles are promising for future use in MRI cell tracking and bioimaging. Recently, water-dispersible MnO Nps were reported as a T1 MRI contrast agent for body organs like brain, the liver and the kidney [15].

The efficient positive contrast agent making is very often addresses, large number of paramagnetic atoms (e.g., Gd^{3+}) within small volumes or confine the contrast agents inside the matrix [16–21]. In the core/shell of Gd_2O_3/NiO Nps, gadolinium oxide can serve as positive contrast agent to reduce T_1 resulting in a brighter signal [13]. In the present work, we demonstrate the spin dynamics studies of NiO encapsulated Gd_2O_3 core–shell Nps employing electron paramagnetic resonance (EPR) spectroscopy which is a powerful tool in the investigation of the magnetic properties and spin dynamics of condensed matter.

2 Experimental

2.1 Materials and Method

The reagent grade of $Gd(NO_3)_3{\cdot}6H_2O$(Alfa Aesar), and $Ni(NO_3)_2{\cdot}6H_2O$ (Alfa Aesar) were used as starting materials. Polyethylene glycol 400 (PEG) was used as solvent, and double distilled water and ethanol were employed for washing.

For the synthesis of NiO and Gd_2O_3 nanoparticles, 0.012 mol/L of $Ni(NO_3)_2{\cdot}6H_2O$ and 0.012 mol/L of $Gd(NO_3)_3{\cdot}6H_2O$ were dissolved separately in 30 mL of PEG under stirring in a round bottomed flask at 100 °C. The clear transparent salt solutions obtained were subsequently heated to 180 °C for 90 min. The resulting greenish brown solution of NiO and brown suspension of Gd_2O_3 were cooled to room temperature, diluted with ethanol and the nanoparticles were separated from the solutions by centrifugation at 10,000 r/min. To remove unreacted precursor and PEG, the sediment materials were dispersed in ethanol and centrifuged for 3 times. The materials obtained after centrifugation were calcined at 600 °C for 2 h in air. To get the nanoparticles of Gd_2O_3/NiO core/shell, NiO shell was grown on the Gd_2O_3 core employing a two step process. Firstly, the as prepared Gd_2O_3 core nanoparticles was dispersed in 25 mL of PEG under sonication for 10 min and then a solution of PEG (15 mL) containing 0.012 mol/L of $Ni(NO_3)_2{\cdot}6H_2O$ was injected into the dispersed nano-core system. After mixing the above solution (using a magnetic stirrer for 15 min), the mixed system was heated at 180 °C for 2 h, and cooled to room temperature, washed, centrifuged and after that calcined at 600 °C for 2 h in air to get Gd_2O_3/NiO core/shell Nps.

2.2 Characterization

To confirm the phase formation, crystal structure and purity of the synthesized samples, the X-ray diffraction (XRD) of the powder samples was taken by powder X-ray diffractometer (Rigaku Miniflex-II) at room temperature. Transmission electron microscopy (TEM) images were obtained using a TECHNAIG^2 TF20ST transmission electron microscope operating at 200 kV. The samples for TEM were prepared by placing a drop of a colloidal acetone solution of the powder sample onto a carbon coated copper grid, and the grid was dried in air. Variable temperature EPR spectra were recorded using a Bruker EMX plus spectrometer operating at X-band ($\nu = 9.43$ GHz) with 100 kHz magnetic field modulation. The temperature was varied from 300 to 110 K and the EPR spectra were recorded while warming the sample. *M-H* hysteresis curves were recorded at room temperature at 6000 ppm (parts per million), using vibration sample magnetometer (VSM).

3 Results and Discussion

3.1 Structural Analysis

In the XRD pattern of Gd_2O_3 core Nps, as shown in Fig. 1a, the major peaks are obtained at $2\theta = 28.50°$, 33.060°, 47.440° and 56.340°, and the corresponding *hkl* planes are (222), (400), (440) and (622), respectively. The nature and position of the above diffraction peaks are characteristics of cubic gadolinium oxide phase (JCPDS 43-1014). Typical XRD pattern of NiO nanoparticles, as shown in Fig. 1b, showing the existence of strong and sharp diffraction peaks at $2\theta = 37.25°$, 43.30° and 63.08°, and the respective crystal planes are (111), (200) and (220). These peaks matched well with those reported results [22–24] (JCPDS 4-0835). Gd_2O_3 and NiO diffraction patterns are observed in the Gd_2O_3/NiO core/shell system, as shown in Fig. 1c, but its diffraction angles are slightly shifted to the higher angle from their bare one. This may be due to the strain existed in core–shell structures which reported by Cao and Banin [25] in epitaxial growth of an InP shell on an InAs core. In the present study, shifting in the diffraction angles at higher values may be due to the very small thickness of the shell material on the core Nps. So the strain from the epitaxial growth of the shell material on the core is strongly affected and is observed as shift in the diffraction pattern of these core–shell Nps.

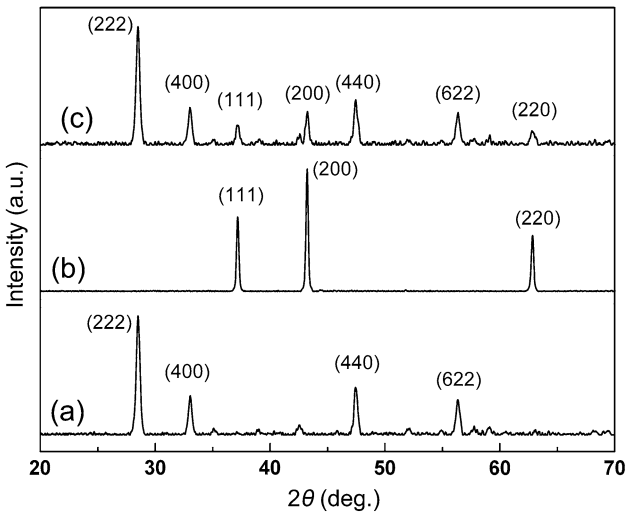

Fig. 1 X-ray diffraction patterns of Gd_2O_3 **a**, NiO **b**, Gd_2O_3/NiO core/shell Nps **c**

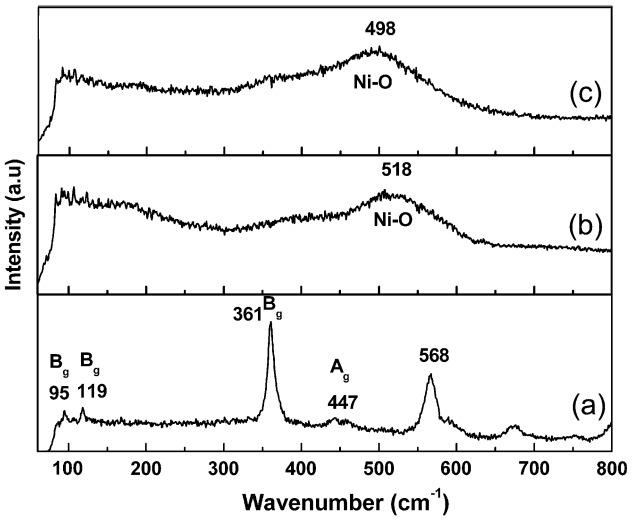

Fig. 2 Raman spectra of Gd_2O_3 **a**, NiO **b**, Gd_2O_3/NiO core–shell Nps synthesized by polyol method **c**

3.2 Raman Studies

In the Raman spectroscopy studies, pure gadolinium oxide Nps clear peaks at 95, 119, 360, and 447 cm^{-1}, as shown in Fig. 2a, indicate that the Gd_2O_3 Nps were in cubic phase [26]. NiO nanoparticle shows broad peak at 518 cm^{-1} (Fig. 2b) due to Ni–O stretching mode [27]. In the case of Gd_2O_3/NiO core–shell nanoparticles (Fig. 2c), NiO peak only observed at 498 cm^{-1} due to the presence of Ni–O stretching mode and the core material peaks were not observed, the shift in lower energy of this peak is due to the increase in the size of core–shell nanoparticles and Gd_2O_3 core material peaks are found to be diminished by the mass effects of the NiO shell material [28].

3.3 TEM Studies

The TEM image obtained for Gd_2O_3/NiO core/shell Nps is shown in Fig. 3a. The average particle diameter is found to be around 35 nm and the structures of these Nps are slightly elongated in shape. The core–shell structure can be clearly seen from the high magnification TEM image (Fig. 3b). It displays the darker part of the Gd_2O_3 core material is encapsulated by the lighter part of NiO shell layer.

3.4 Magnetic Characterizations

3.4.1 Vibrating Sample Magnetometer (VSM)

The magnetic hysteresis for the NiO and Gd_2O_3/NiO core–shell nanoparticles at room temperature obtained using VSM is presented in Fig. 4. It is observed that the magnetization of the NiO nanoparticles (Fig. 4a) increases rapidly with applied magnetic field and is not saturated even at 20 kOe (1,591.56 kA/m) and the value of coercivity is found to be 187 Oe (14.88 kA/m). The NiO is a typical antiferromagnetic material in the bulk form but we observed coercivity in present case indicates the uncompensated surface spins causing a change in the magnetic order of NiO Nps [29, 30]. In the case of NiO encapsulated Gd_2O_3 core–shell nanoparticles (Fig. 4b), it reveals that the magnetization increases rapidly without reaching saturation in a field at 16 kOe (1,273.25 kA/m) and the H_c value is 85 Oe (6.764 kA/m). This linear *M-H* behavior is characteristics of a typical diamagnetic material. This decreased magnetic property of Gd_2O_3/NiO core–shell nanoparticles may be due to the non-magnetic contribution of Gd_2O_3 core at room temperature. The observed value of the magnetic moment is very low and the H_c value is 85 Oe (6.764 kA/m) for the core–shell Nps and this may be associated with surface spins arising from the nanoscale thickness of NiO shell material.

3.4.2 Electron Paramagnetic Resonance (EPR) Studies

Typical first derivative EPR spectra obtained for the Gd_2O_3/NiO core/shell nanoparticles in the temperature range of 110–300 K are shown in Fig. 5. The spectra reveal a single broad signal from 300 to 200 K. In addition to the broad signal, a small narrow signal corresponding to a resonance field of 0.394 T is present when the temperature is further decreased to 150 and 110 K respectively. The appearance of the additional small signal at low temperature may be due to the anisotropy present in the sample induced by the strain in

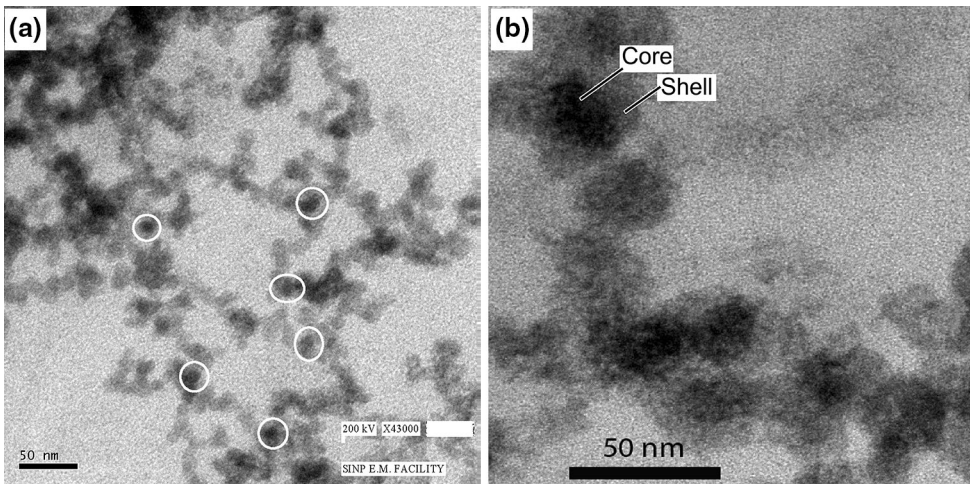

Fig. 3 TEM images of Gd_2O_3/NiO core/shell Nps with different magnifications of 43,000× **a**, 71,000× **b**

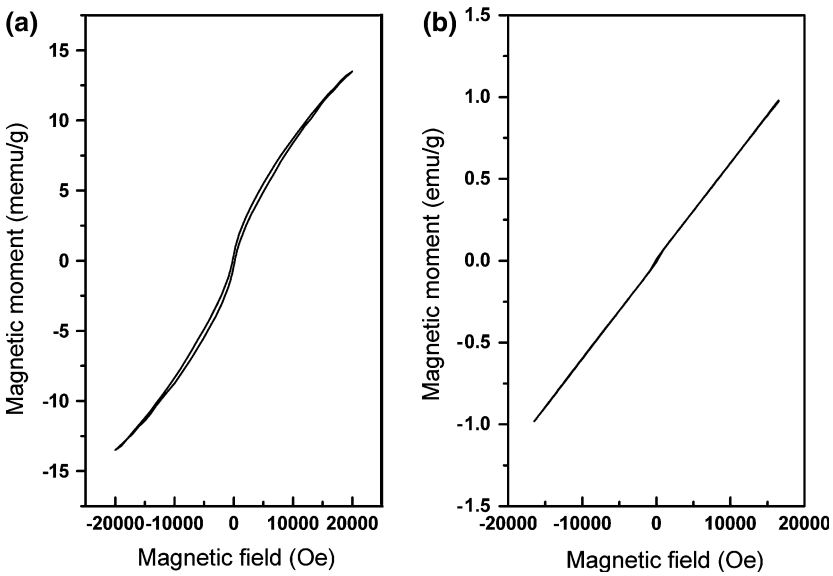

Fig. 4 Room temperature hysteresis curves obtained through VSM studies: **a** NiO; **b** Gd_2O_3/NiO core/shell Nps

the particles which is associated with the large surface area of the nanoparticles [31]. When the temperature is increased, this anisotropy energy is suppressed by the thermal energy and we get the homogeneous broad signal in the temperature range of 200–300 K.

The peak-to-peak linewidth (ΔH_{pp}) is found to increase rapidly with the increment of the temperature (Table 1). This usually is caused in the core–shell nanoparticles by the magnetic dipole interactions at high temperatures. When the temperature is decreased, the average anisotropic field of the present sample may dominate the interparticle dipolar interaction, thus may lead to the reduction in the width producing relatively a narrow signal [32]. The ΔH_{pp} values for NiO encapsulated Gd_2O_3 Nps are larger than the reported bare Gd_2O_3 Nps at room temperature [13].

The energy between two adjacent degenerate spin energy levels, ΔE, has the same behavior of the linewidth. The reduction of the linewidth may cause a reduction in the separate energy ΔE. The value of ΔE is given by the relation $\Delta E = h\nu = g\mu_B H_0$ [33]. The peak-to peak line width (ΔH_{pp}) and g-values are decreasing with the decrement of the temperature (Table 1), which depends upon two main factors namely magnetic dipole interactions among the particles and exchange interaction between the ions. Strong dipole interaction gives a large ΔH_{pp} and strong superexchange interaction produces a small ΔH_{pp} [32]. In core–shell magnetic nanosystem interfacial exchange coupling between core and shell region also plays as an important parameter. Ong et al. [34] reported that the exchange coupling between core and shell region is strong under low temperature conditions.

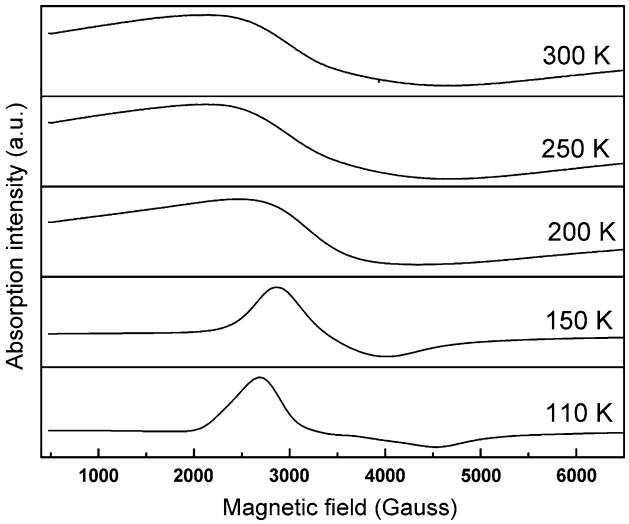

Fig. 5 EPR spectra of Gd_2O_3/NiO core/shell Nps at low temperatures of 300–110 K

Table 1 EPR parameters of Gd_2O_3/NiO core/shell nanoparticles at different temperatures

Temperature (K)	ΔH_{pp} (Gauss)	g-value	T_2 (ps)	T_1 (ps)	Number of spin
110	1,844	2.09	17.0	8.51	1.70×10^{14}
150	1,151	1.98	28.7	4.51	1.11×10^{14}
200	1,877	2.05	17.0	81.60	2.81×10^{13}
250	2,522	2.13	12.2	12.20	2.88×10^{13}
300	2,562	2.13	12.0	12.40	1.92×10^{13}

If this temperature is decreased in this core/shell nanoparticle, anisotropy field of the nanoparticles and interfacial exchange coupling between core and shell region will greatly affect the ΔH_{pp} and g-values. At higher temperatures, spin direction between the antiferromagnetic NiO shell and the nonmagnetic Gd_2O_3 core are different, and in this condition, interfacial exchange coupling between the core and shell regions is not too significant [35]. Sunderesan et al. [36] found that the non magnetic metal oxide nanoparticles show the ferromagnetic moment because of the presence of defects on the surface of the material. In the present case at low temperature, disordered spins on the gadolinium oxide core surface coupled with interface of shell material results in the arising of net magnetic moment from 150 to 110 K. The interfacial roughness between the core and the shell region will be larger when the core surface disorder increases. This increasing interfacial roughness leads to a greater degree of uncompensated spin at the interface [35], and hence a larger degree of unidirectional coupling between antiferromagnetic shell (NiO) and non magnetic core (Gd_2O_3) from 150 K in Gd_2O_3/NiO core–shell nanoparticle system occurs. The g-factor value increases at 110 K which may be due to the strong interfacial exchange coupling between the core and shell region.

It is known that there are two relaxation processes in EPR system: viz. spin–lattice and spin–spin relaxation. If the line width of the EPR spectrum is determined by spin–spin relaxation, the ΔH_{pp} will increase rapidly as the temperature decreases [37], but we get only opposite trend in our system. Therefore, it may not be associated with the spin–spin relaxation that plays a dominant role but the other mechanism, such as spin–lattice relaxation should be operative. If the involved spins are like (parallel) the magnetic exchange interaction causes a broadening of the resonance lines, at higher temperature. On the contrary, if the magnetic exchange takes place between unlike (anti-parallel) spins a narrowing resonance lines is caused at higher temperatures. The observed broadening of the EPR peaks at higher temperatures in the present case may be attributed to the exchange interaction between the like spins. Due to the spin–lattice relaxation characteristics of Gd_2O_3/NiO core–shell Nps, it can be used as a T_1 contrast agent in the MRI application [20, 21]. The Homogeneous broadening and the peak-to-peak line width of the EPR spectra are used to estimate the spin–spin relaxation time (T_2) and spin–lattice relaxation time (T_1) [38]:

$$1/T_2 = \pi g \mu_B \Delta H/h, \tag{1}$$

$$T_1 = 1/2\gamma^2 T_2 H_r, \tag{2}$$

where ΔH is the full-width-at-half-maximum (FWHM) of the absorption curve ($\Delta H = \Delta H_{pp}$), γ is the gyromagnetic ratio, and T_1 and T_2 are calculated using Eqs. (1) and (2) and the other needed values are given in Table 1. The relaxation time estimated from the EPR studies does not show any regular trend with the temperature.

The EPR spin number is the area under the EPR absorption curve, which is proportional to the number of unpaired spins in the sample. The EPR spin number is evaluated from the product of square of line width and peak to peak height ($\Delta H_{pp}^2 h$) [39]. It is seen from the Table 1 that the lowest spin number (1.92×10^{13}) observed at 300 K, and the spin number for both the temperatures 250 and 200 K are the same and is observed as 2.8×10^3. A sudden increment of EPR signal intensity is observed at 150 and 110 K. This may be associated with the uncompensated spin arising at the interface between the core and shell region because of the fact that the exchange coupling effect at very low temperature resulted in the larger Ns value as observed for the temperature below 200 K.

4 Conclusion

Well-crystalline Gd_2O_3, NiO and Gd_2O_3/NiO (core/shell) nanoparticles have been successfully synthesized by polyol process. Core–shell structures of the Gd_2O_3/NiO Nps are

analyzed by XRD and Raman spectroscopic studies. The average particle size of the core/shell nanoparticles was found to be <35 nm through TEM studies. The temperature dependent EPR spectra of magnetic core–shell nanosystems were scanned from 110 to 300 K. When temperature below 200 K, the spectra showed an additional small peak associated with the anisotropy in the sample induced by the strain in the particle of large surface area nanoparticles. The g-factor and N_s decreased with decreasing temperature from 300 to 200 K and increased at very low temperatures. The results may be due to the dominance of anisotropy field and interfacial exchange coupling between the core and shell region which is usually significant at very low temperature in this NM/AFM core/shell nanosystem. Peak-to-peak line width increased with the increase of temperature indicating spin–lattice relaxation operating in this Gd_2O_3/NiO core/shell nanosystems. Electron spin relaxation time of Gd_2O_3 Nps could be changed by encapsulation of nanoscale NiO shell material. Further experiments are planned to study if NiO encapsulated Gd_2O_3 core–shell Nps have an increased relaxivity in water solutions at clinical relevant magnetic field strengths.

Acknowledgments This work was financially supported by the Department of Science and Technology (DST-PURSE) Government of India, New Delhi in the form of fellowship.

References

[1] S. Krol, R. Macrez, F. Docagne, G. Defer, S. Laurent, M. Rahman, M.J. Hajipour, P.G. Kehoe, M. Mahmoudi, Chem. Rev. **113**, 1877 (2013)
[2] V. Castranova, P.A. Schulte, R.D. Zumwalde, Acc. Chem. Res. **46**, 642 (2013)
[3] K. Ariga, Q. Ji, J.P. Hill, Y. Bando, M. Aono, NPG Asia Mater. **4**, e17 (2012)
[4] K. Ariga, T. Mori, J.P. Hill, Adv. Mater. **24**, 158 (2012)
[5] J.N. Coleman, Acc. Chem. Res. **46**, 14 (2013)
[6] K. Ariga, A. Vinu, Y. Yamauchi, Q. Ji, J.P. Hill, Bull. Chem. Soc. Jpn. **85**, 1 (2012)
[7] H. Zeng, S. Sun, J. Li, Z.L. Wang, J.P. Liu, Appl. Phys. Lett. **85**, 792 (2004)
[8] V.S. Maceira, M.A. Correa-Duarte, Adv. Mater. **19**, 4131 (2007)
[9] N. Sounderya, Y. Zhang, Recent Pat. Biomed. Eng. **1**, 34 (2008)
[10] M.Q. Chu, X. Song, D. Cheng, S.P. Liu, J. Zhu, Nanotechnology **17**, 3268 (2006)
[11] W. Fu, H. Yanga, Q. Yua, J. Xua, X. Panga, G. Zou, Mater. Lett. **61**, 2187 (2007)
[12] C.N. Thian, COSMOS **8**, 103 (2012)
[13] H. Gustafsson, M. Ahren, F. Soderlind, J.M.C. Gallego, P.O. Kall, P. Nordblad, P.O. Westlund, K. Uvdal, M. Engstrom, J. Phys. Chem. C **115**, 5469 (2011)
[14] M. Ahren, L. Selegard, A. Klasson, F. Soderlind, N. Abrikossova, C. Skoglund, T. Bengtsson, M. Engstrom, P.O. Kall, K. Uvdal, Langmuir **26**, 5753 (2010)
[15] H.B. Na, J.H. Lee, K. An, Y.I. Park, M. Park, I.S. Lee, D.H. Nam, S.T. Kim, S.H. Kim, S.W. Kim, K.H. Lim, K.S. Kim, S.O. Kim, T. Hyeon, Angew. Chem. Int. Ed. **46**, 1 (2007)
[16] M.A. Fortin, R.M. Petoral Jr, F. Soderlind, A. Klasson, M. Engstrom, T. Veres, P.O. Kall, K. Uvdall, Nanotechnology **18**, 395501 (2007)
[17] J.L. Bridot, A.C. Faure, S. Laurent, C. Riviere, C. Billotey, B. Hiba, M. Janier, V. Josserand, J.L. Coll, L.V. Elst, R. Muller, S. Roux, P. Perriat, O. Tillement, J. Am. Chem. Soc. **129**, 5076 (2007)
[18] F. Evanics, P.R. Diamente, F.C.J.M. van Veggel, G.J. Stanisz, R.S. Prosser, Chem. Mater. **18**, 2499 (2006)
[19] H. Hifumi, S. Yamaoka, A. Tanimoto, D. Citterio, K. Suzuki, J. Am. Chem. Soc. **128**, 15090 (2006)
[20] H.B. Na, I.C. Song, T. Hyeon, Adv. Mater. **21**, 2133 (2009)
[21] H.B. Na, T. Hyeon, J. Mater. Chem. **19**, 6267 (2009)
[22] D. Tao, F. Wei, Mater. Lett. **58**, 3226 (2004)
[23] H. Guan, C. Shao, S. Wen, B. Chen, J. Gong, X. Yang, Inorg. Chem. Commun. **6**, 1302 (2003)
[24] H. Jiao, Nano-Micro Lett. **3**(3), 166 (2011)
[25] Y.W. Cao, U. Banin, J. Am. Chem. Soc. **122**, 9692 (2000)
[26] C. Le Luyer, A. Garcia-Murillo, E. Bernstein, J. Mugnier, J. Raman Spectrosc. **34**, 234 (2003)
[27] S.I. Cordoba-Torresi, A. Hugot-Le Goff, S. Joiret, J. Electrochem. Soc. **138**, 1554 (1991)
[28] E.B. Santos, J.M. de Souza e Silva, I.O. Mazali, Vib. Spectrosc. **54**, 89 (2010)
[29] R.H. Kodama, S.A. Makhlouf, A.E. Berkowitz, Phys. Rev. Lett. **79**, 1393 (1997)
[30] M. Ghosh, K. Biswa, A. Sundaresen, C.N.R. Rao, J. Mater. Chem. **16**, 106–111 (2006)
[31] V. Tsurkan, M. Lohmann, H.A. Krug-von-Nidda, A. Loidi, S. Horn, R. Tidecks, Phys. Rev. B **63**, 125209 (2001)
[32] L. Li, G. Li, R.L. Smith, H. Inomata, Chem. Mater. **12**, 3705 (2000)
[33] J.F. Raber, *Experimental Methods in Polymer Chemistry-Physical Principal and Applications* (Wiley, New York, 1980), p. 332
[34] Q.K. Ong, A. Wei, X.M. Lin, Phys. Rev. B **80**, 134418 (2009)
[35] R.F.L. Evans, D. Bate, R.W. Chantrell, Phys. Rev. B **84**, 092404 (2011)
[36] A. Sundaresan, R. Bhargavi, N. Rangarajan, U. Siddesh, C.N.R. Rao, Phys. Rev. B **74**, 161306 (2006)
[37] G. Dixit, J.P. Singh, R.C. Srivastava, H.M. Agarwal, J. Magn. Magn. Mater. **324**, 479 (2012)
[38] J.P. Singh, R.C. Srivastava, H.M. Agarwal, R.P.S. Kushwaha, J. Nanosci. Nanotechnol. **7**, 21 (2008)
[39] K.H. Wu, Y.C. Chang, H.B. Chen, C.C. Yang, O.N. Horng, J. Magn. Magn. Mater. **278**, 156 (2004)